On the measurement of stability parameter over complex mountainous terrain

Elena Cantero[1], Javier Sanz[1], Fernando Borbón[1], Daniel Paredes[2], Almudena García[3]

[1] National Renewable Energy Centre (CENER), Sarriguren, Spain

[2] Iberdrola, Madrid, Spain

[3] Smart Cities Institute, Universidad Pública de Navarra (UPNA), Spain

Correspondence to: Elena Cantero (ecantero@cener.com)

Abstract. Atmospheric stability has a significant effect on wind shear and turbulence intensity, and these variables, in turn, have a direct impact on wind power production and loads on wind turbines. It is therefore important to know how to characterize atmospheric stability in order to make better energy yield estimation in a wind farm.

Based on research grade meteorological mast at Alaiz (CENER's Test Site in Navarre, Spain) named MP5, this work compares and evaluates different instrument set-ups and methodologies for stability characterization, namely: tThe Obukhov parameter $\zeta = z/L$, which can be measured locally with the use of a sonic anemometer, and the bulk Richardson number have been studied based on two temperature and one wind speed measurements. The methods are examined considering their theoretical background, implementation complexity, instrumentation requirements, and practical use in connection with to wind energy applications. The sonic method provides a more precise local measurement of stability while the bulk Richardson is a simpler, robust and cost-effective technique to implement in wind assessment campaigns. Using the sonic method as a benchmark, it is shown that to obtain reliable bulk Richardson measurements in onshore sites it is necessary install one of the temperature sensors close to the ground where the temperature gradient is stronger.

Bulk Richardson number, which is based on one height wind speed measurement and two temperature measurements, is sometimes calculated using values from any two temperature levels without taking into account that one of the measurements would be representative of surface conditions. With the data available in MP5, it will be shown how this approximation is not correct to obtain an adequate stability characterization.

1. Introduction

The vertical wind profile and the turbulence intensity in the atmospheric boundary layer (ABL) are two of the main physics aspects driving wind energy production and turbine loads. the features that most affect the wind energy generation. The vertical wind profile is especially important since rotors are getting bigger and hub heights are getting higher making it invaluable to know the wind speed at hub height. The vertical wind profile shape and turbulence intensity can directly influence wind turbine production but also wind turbine loads, affecting the wind turbines lifetime. The wind profile because given the growing hub heights and rotor sizes of the modern wind turbines it affects the wind turbine production and loads; and the turbulence intensity because it induces loads that the wind turbine will support over its design lifetime. Despite the fact that the IEC standard (IEC61400-1 (ED4) 2019, 2019) specifies a power law vertical model independent of atmospheric stability to perform load calculations, the dependence of this and, in turn, the turbulence intensity with atmospheric stability is widely demonstrated (Emeis, 2013; Lange et al., 2004b; Peña and Hahmann, 2012). In addition several studies have demonstrated the impact of atmospheric stability on wind resource assessment (Lange et al., 2004a), wind turbine power curves and Annual Energy Production (AEP) calculations (Martin et al., 2016; Schmidt et al., 2016); wind turbine loads (Kelly et al., 2014; Sathe et al., 2013) and wind turbine wakes (Abkar and Porté-Agel, 2015; Hansen et al., 2010; Machefaux et al., 2016). This is why the wind industry is developing models and methods to include the effect of atmospheric stability in the layout design and energy yield assessment. These methodologies and models require the characterization of the probability distribution of atmospheric stability at each site. Therefore different methods and parameters are used to describe atmospheric stability without an industry-wide convention about which one is the most appropriate.

According to Monin and Obukhov similarity theory (MOST) (Foken, 2006; Monin and Obukhov, 1954) stability can be estimated in terms of inverse of Obukhov length that can be calculated with vertical fluxes of heat and momentum obtained with the eddy covariance method. To obtain the necessary high-frequency measurements of

wind speed vector components and temperature, sonic anemometers are used, which is why this calculation method is called "sonic method".

Another measure for stability is the Richardson number that as Bardal (Bardal et al., 2018) explains according to Stull book (Stull, 1989) has several formulations: the flux Richardson number, gradient Richardson number and bulk Richardson number. The latter is based on one height wind speed measurement and two temperature measurements, one from the air at one height and the other from the ground or water surface.

In the wind energy context some studies have been done about how to measure the stability and their influence in the turbulence intensity and vertical wind profile. However, most of these studies have been carried out in offshore sites (Peña and Hahmann, 2012; Sanz Rodrigo et al., 2015; Sathe et al., 2011) finding relationships (Grachev and Fairall, 1997) between the Obukhov length and the Richardson bulk number that, facilitate the characterization of stability without the need of sonic anemometer. This is convenient, because although the sonic anemometer has many advantages (Cuerva et al., 2006), This is convenient to avoid thethey added complexity, in terms of use and data management, and cost, ten times higher than cup anemometers, of these instruments into the long-term site assessment campaigns.

For onshore sites there are few studies that analyse how to characterize atmospheric stability and those that exist are on simple topography in coastal areas (Bardal et al., 2018).

Although the behaviour of wind flow over complex terrain is widely studied, as Finnigan summarizes in (Finnigan et al., 2020) and there are recent publications about the influence of atmospheric stability in wind farms located in complex terrain (Han et al., 2018; Radünz et al., 2020, 2021); there are no references that analyse in detail how to characterize atmospheric stability according to different instrumentation requirements.

Measuring atmospheric stability in complex terrain has some challenges (compared to flat terrain), one of them is the fact that the MOST is developed for horizontally homogeneous and flat terrain and in complex terrain vertical wind speed can be due to stability or sloping terrain, therefore, vertical fluxes will be "contaminated" by terrain effects. This can be mitigated by using good measurement practices (data quality, coordinate systems and post processing options) (Stiperski and Rotach, 2015).

This study presents atmospheric stability characterization from one mountainous site obtained using two methods: sonic method and the Richardson bulk number. Measurements of different heights have been used to see the influence of this parameter on the results

The place used in this study meets the characteristics of a typical complex terrain site for wind energy deployment. The 118 m high MP5 reference meteorological mast, as is explained in other articles by Sanz (Sanz Rodrigo et al., 2013) and Santos (Santos et al., 2020), is equipped with wind (cup and 3D sonic anemometer) and temperature measurements distributed along six vertical levels: 2, 40, 80, 90, 100 and 118 m above the ground level (a.g.l), enabling the comparison between Richardson bulk number and the sonic method to evaluate atmospheric stability.

Special focus is given to explaining the post-processing methodologies to derive stability from raw data considering fast-response sonic anemometer in a complex terrain.

2. Atmospheric stability definitions

2.1 The Obukhov length

Monin and Obukhov (M-O) (Monin and Obukhov, 1954) introduced the Obukhov length L to characterize atmospheric stability, which is proportional to the height above the surface at which the production of turbulent energy from buoyancy dominates over mechanical shear production of turbulence (Stull, 1989), and it is defined as:

$$L = -\frac{u_*^3}{\kappa \frac{g}{\Theta_0} \overline{w'\theta'}}$$
(1)

Where $g = 9.81\ ms^{-2}$ is the acceleration due gravity, $\kappa = 0.41$ is the von Karman constant, $u*$ is the friction velocity, Θ_0 is the surface potential temperature and $\overline{w'\theta'}$ is the heat flux. The dimensionless height $\zeta = z/L$ is used as stability parameter, where $\zeta < 0$ indicates unstable, $\zeta > 0$ stable and $\zeta = 0$ neutral conditions.

Table 1 shows the Sorbjan & Grachev (Sorbjan and Grachev, 2010) stability classification proposing, they identify four regimes in the stable conditionsboundary layer. This classification is also followed by Sanz (Sanz

Comentario [ECN5]: Answer RC2 specific comments.

Comentario [ECN6]: Answer RC2 Technical corrections

Comentario [ECN7]: Answer RC2 Technical corrections.

Comentario [ECN8]: Answer RC2 Technical corrections.

Rodrigo et al., 2015) assuming a symmetric classification in the unstable range. Sanz Rodrigo *et al.* shift the "extremely unstable and /stable" regime limit to |ζ| = 1 in order to avoid contamination of the large scatter found in the high ends of the scale to the "very unstable and/stable" class. An additional limit is added at |ζ|=0.2 to give higher resolution in the most frequent stability range. For consistency, we shall adopt the same classification used in (Sanz Rodrigo et al., 2015) to facilitate the comparison with offshore conditions.

Table 1 Classification of atmospheric stability adapted from (symmetric for the unstable range) (Sorbjan and Grachev, 2010).

Stability Class	Stability parametereter ζ = z/L
extremely unstable (xu)	ζ <-1
very unstable (vu)	-1 < ζ < -0.6
unstable (u)	-0.6 < ζ <- 0.2
weakly unstable (wu)	-0.2 < ζ < -0.02
near-neutral (n)	0 < ζ < 0.02
weakly stable (ws)	0.02 < ζ < 0.2
stable (s)	0.2 < ζ < 0.6
very stable (vs)	0.6 < ζ < 1
extremely stable (xs)	ζ > 1

Using sonic anemometers and eddy covariance technique, the Obukhov length can be obtained. In this way, stability is evaluated locally based on turbulent fluxes averaged over periods from minutes to one hour to integrate the kinetic energy in the microscale turbulence range.

Sonic anemometer can be used in complex terrain to derive the local Obukhov length. Following the planar fit method of Wilczak et al. (Wilczak et al., 2001), momentum fluxes should be calculated in the mean streamline plane and heat fluxes in the true vertical coordinate system. If the streamline plane can be known a priori, from a wind direction sector with uniform slope, the planar fit method can be used to infer the mounting tilt angle and correct for it to reduce the uncertainty on the vertical fluxes.

2.2 Bulk Richardson number

The bulk Richardson number Ri_b is a form of the Richardson number that is widely used for characterizing stability for its simplicity, defined in terms of a (potential) potential temperature difference and a single velocity level:

$$Ri_b = -\frac{gz\Delta\Theta}{\Theta_0 \overline{\overline{U}}^2} \tag{2}$$

Where, as proposed Sanz *et al.* in (Sanz Rodrigo et al., 2015), the height z is taken here as the mean height between the two levels of temperature and $\Delta\Theta$ is derived from the water-air or surface-air temperature difference.

As Bardal *et al.* propose in (Bardal et al., 2018) propose the general empirical relations from Businger et al. (Businger et al., 1971) slightly modified by Dyer (Dyer, 1974) have been used to relate ζ with the Rib:

$$\xi = \begin{cases} Ri_b, & Ri_b < 0 \\ \frac{Ri_b}{1-5Ri_b}, & 0 < Ri_b < 0.2 \end{cases} \tag{3}$$

Alternatively Ri_b can be used directly to do a stability classification. (Mohan, 1998) has proposed a seven classes of stability classification methodology (Table 2) which has been accepted by the scientific community as it was shownAlternatively by Ri_b can be used directly to do a stability classification, according to Mohan (Mohan, 1998) which classification is used in literature (Ruisi and Bossanyi, 2019), based on seven classes of stability (Table 2).

Table 2 Classification of atmospheric stability (Mohan, 1998).

Stability Class	Stability parametereter Ri_b
Very unstable	Rib < -0.023
Unstable	-0.023 ≤ Rib < -0.011
Weakly unstable	-0.011 ≤ Rib < -0.0036
Neutral	-0.0036 ≤ Rib < 0.0072

Weakly stable	$0.0072 \leq Rib < 0.042$
Stable	$0.042 \leq Rib > 0.084$
Very stable	$Rib \geq 0.084$

3. The Alaiz site

The MP5 mast is located (42º41.7' N, 1º33.5' W) at the top of Alaiz mountain in the region of Navarre (Spain), around 15 km SSE from Pamplona in the CENER's experimental wind farm. The prevailing wind directions are from the North and from the South. To the North there is a large valley at around 700 m lower altitude. To the South, complex terrain is found with the presence of some wind farms; the closest one situated 2 km behind the row of six wind turbine stands of the test site (see Fig. 1). As it is explained by (Sanz Rodrigo et al., 2013) the wakes from this wind farm can be considered well mixed with the boundary layer flow in most conditions so additional turbulence it is not expected in MP5 due wakes from neighbour wind farms.

Besides MP5 meteorological mast there are four other reference met masts (MP0, MP1, MP3 and MP6), all of them 118 m tall.

The test site started operating in 2009 with the site calibration procedures. The first wind turbines were installed in the summer of 2011. The standard configuration of each mast is designed for multi-megawatt wind turbine testing and includes sonic and cup anemometer, wind vanes and temperature/humidity measurements. Replicated cup anemometers are situated 2 m below the reference ones.

The mast MP5 is 118 m high lattice permanent mast with nine measurement levels with booms oriented to the West (263º) and the East (83º). Wind speed and wind direction are measured at five levels (118, 102, 90, 78 and 40 m) with cups anemometer (oriented to the West) and wind vanes (oriented to the East); while sonic anemometer are installed at 115.5, 75.5 and 39.5 m (oriented to the West). Temperature and relative humidity are measured at five levels (113, 97, 81, 38 and 2 m) and pressure at 2 m high.

The instrumental set-up is compliant with IEC 61400-12-1(IEC61400-12-1 (ED1) 2005-12, 2005) with MEASNET cup anemometer calibration (Measnet, 2009) and with ENAC accreditation according to UNE-EN ISO/IEC 17025.

The data acquisition system consist in a real-time controller CompactRIO from National Instruments with 128 MB DRAM and 2 GB storage embedded in a chassis in connection with 8 modules of digital and analogical data acquisition. All connected to an Ethernet network.

The rate sample is 5 Hz for cup anemometer (Vector A100LK) and 20 Hz for sonic anemometer (METEK USA-1), wind vanes (Thies Compact), pressure (Vaisala PTB100A), and humidity temperature sensor (Ammonit P6312).

Figure 2 shows the wind rose at the MP5 site, from the period between July 2014 to June 2015. It presents a bidirectional wind climate, with prevailing winds from the north-northwest sector (330–360, 32% of total) and the south southeast sector (150–180, 28% of total).
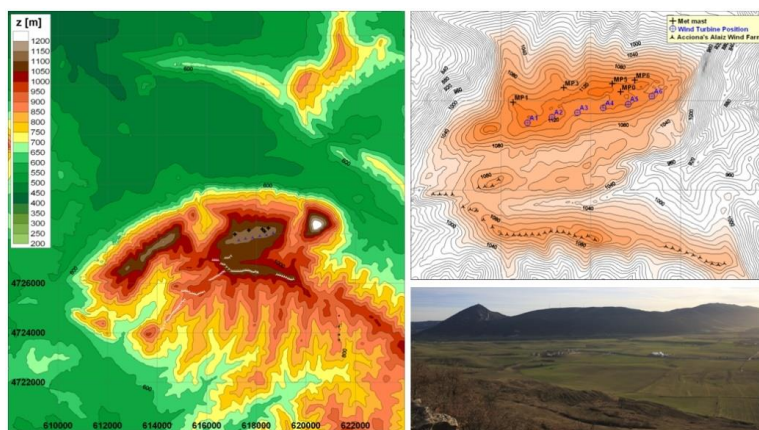
Figure 1 Alaiz elevation map, close-up of the test site and view from the upstream ridge to the North.
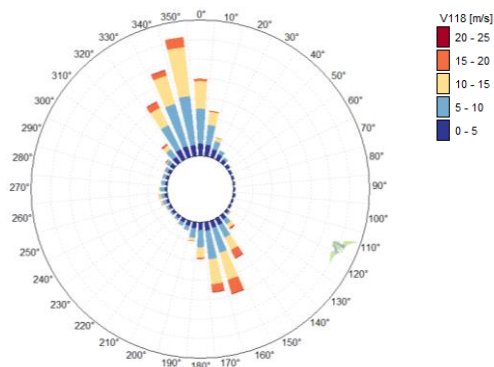
161 **Figure 2 Wind rose of 10 min wind speeds observed by MP5 at 118m for the reference period (July 2014–June 2015).**

162 ## 4.   Methodology

163 In the present work, a one year period (1st July 2014 to 30th June 2015) is analyzed. ~~Measurements~~ Flux
164 measurements from the sonic anemometer at 115.5, 75.5 and 39.5 m are used to calculate de Obukhov length L,
165 while conventional sensors (wind direction, relative humidity, air pressure and temperature) are used to estimate the
166 bulk Richardson number.

Comentario [ECN20]: Answer RC2 Technical corrections.

167 ### 4.1 Data quality control

168 Before calculating stability parameter all data are checked for data quality.

169 Data from conventional sensors (wind direction, relative humidity, air pressure and temperature) have been
170 processed following Brower (Brower, 2012). It consists on checking the completeness of the collected data and
171 applying several test (range, relational and trend). After filtering for quality-control purposes, the conventional
172 sensors provide horizontal wind speeds, directions, relative humidity, pressures and temperatures availabilities
173 greater than 85% at all levels during the evaluation period.

174 For sonic anemometer there are a lot of procedures (Aubinet et al., 2012) and test criteria for quality control of
175 turbulent time series and studies about the impact in the results of this procedures (Stiperski and Rotach, 2015).

176 High-frequency raw data often contain impulse noise, that is, spikes, dropouts, constant values, and noise. Spikes
177 in raw data can be caused by instrumental problems, such as imprecise adjustment of the transducers of ultrasonic
178 anemometer, insufficient electric power supply, and electronic noise, as well as by water contamination of the
179 transducers, bird droppings, cobwebs, etc., or rain drops and snowflakes in the path of the sonic anemometer.

180 Several spikes in wind speed have been detected in the raw sonic anemometer data. Therefore, a de-spiking filter
181 is applied based on the change in wind speed from each data point to the next and taking into account the physical
182 limits according to sensor specifications. Data points are removed if they are preceded and followed by changes
183 exceeding the lowest 99% of all changes. After filtering the spikes, the sonic anemometer provide wind speed and
184 temperature availabilities greater than 80% in the three sonic anemometer.

185 ### 4.2 Eddy Covariance method

186 The operating principles of sonic anemometer are described by different authors (Aubinet et al., 2012; Cuerva et al.,
187 2003; Kaimal and Businger, 1963; Kaimal and Finnigan, 1994; Schotanus et al., 1983). The sonic anemometer
188 output provides three wind components in an orthogonal axis system and sonic temperature. The relation between
189 sonic temperature and absolute real temperature is given by ~~Kaimal & Gaynor~~ (Kaimal and Gaynor, 1991).

190 High frequency data from sonic anemometer have been processing to obtain 10 minutes databases that include
191 turbulent fluxes of energy, mass, and momentum with the eddy covariance technique (Aubinet et al., 2012)(Burba,
192 2013; Burba and Anderson, 2010; Geissbühler et al., 2000).

193 The main requirements for instruments and data acquisition systems used for eddy covariance data are their
194 response time to solve fluctuations up to 10 Hz. This means that the sampling frequency has to be high enough to

195 cover the full range of frequencies carrying the turbulent flux, leading usually to a sampling rate of 10–20 Hz. In the
196 test case in this report 20 Hz is the sample rate for the sonic anemometer.

197   The transformation of high-frequency signals into means, variances, and covariances requires different steps
198 (Aubinet et al., 2012; Stiperski and Rotach, 2015), in this study the next steps ~~has~~ have been proposed:

199 1. Quality Control of raw data, explained in point 4.1.2
200 2. Coordinate Rotation, transformation of coordinate systems, from the original axes based on the anemometer
201   output to the streamline terrain-following system, based on the Planar Fit Method (PFT) (Richiardone et al.,
202   2008; Wilczak et al., 2001). Momentum fluxes and heat fluxes have been calculated with respect to the
203   streamline terrain-following coordinate system. Figure 3 shows the steps to rotate the axes from mounting
204   coordinates to streamline coordinates.
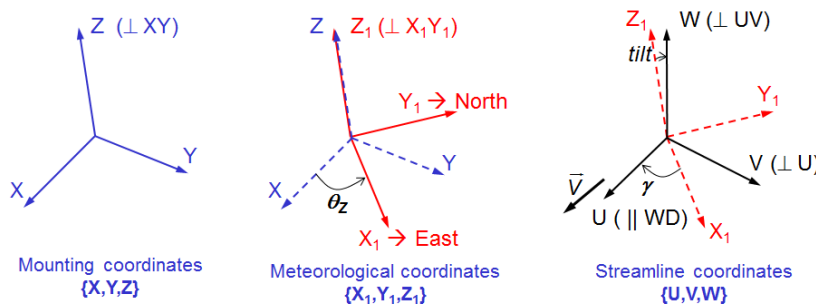
205 **Figure 3 Schematic description for the rotation process.**

206 **3.** Variance and Covariance Computation, apply eddy covariance technique for calculation of vertical turbulent
207   fluxes (heat and momentum). It corresponds to the calculation of the covariance of the fluctuations of the vertical
208   velocity with the quantity Φ (temperature for heat, velocity components for momentum).

$$F_\phi = \overline{w'\phi'} = \overline{w\phi} - \overline{w}\,\overline{\phi} = \frac{1}{N-1}\left[\sum w'\phi' - \frac{1}{N}\left(\sum w'\right)\left(\sum \phi'\right) \right] \tag{4}$$

209
210   N denotes the number of samples considered for the short averaging period T over which the flux is
211 calculated (from 5 to 60 minutes). N has to be long enough to ensure statistical convergence and short enough to
212 assume stationarity (in complex terrain difficult to fulfil both criteria). In this work a 10 minutes averaging period
213 has been selected.

214   In the MP5's sonic anemometer, at 115.5, 75.5 and 39.5 m height, moreover the temperatures, the variables
215 recorded are: the module of wind speed vector, the direction and vertical component (z). These values are projected
216 to meteorological coordinates to obtain the three components of wind speed vector (x, y, z) after being filtered the
217 transformation of high-frequency signals into means, variances, and covariances has been done.

218   The 10 minutes values of wind speed from sonic anemometer after applying steps 1 to 3 are checked and some
219 non-valid data are detected. As in conventional sensors these invalid data are due to icing effects so they are filtered.

220 **4.4 Stability assessment**

221 MP5's sonic anemometer ~~allowing~~ allow evaluating stability based on the local Obukhov length at different heights.
222 This will be the benchmark method since it is directly obtained from the measurements without introducing any
223 assumptions or empirical relationships. The bulk Richardson number is evaluated as an alternative methodology
224 since it follows easier instrumentation set-up and post-processing, and for offshore places has presented good results
225 (Sanz Rodrigo, 2011; Sanz Rodrigo et al., 2015).

226 **4.4.1 Sonic method**

227 To obtain the stability parameter $\zeta = z/L$, as it was explained before, sonic anemometer measurements are rotated to
228 the mean streamline coordinate system using the planar fit method to guarantee that the mean streamline plane will
229 be parallel to the terrain surface. After this, variances and covariances of detrended velocity and sonic temperature
230 perturbations are computed using the eddy covariance technique over high frequency timescale. Then, turbulent
231 fluxes are obtained by averaging the covariances over a period of 10 minutes.

Comentario [ECN21]: Answer RC2 Technical corrections.

Comentario [ECN22]: Answer RC2 Specific comments

Comentario [ECN23]: Answer RC2 Technical corrections.

In complex terrain, the hypothesis of a homogeneously horizontal surface layer is not fulfilled so the applicability of Monin and Obukhov similarity theory (MOST) to complex terrain conditions is not obvious. This signify that for the complex sites as Alaiz the theory is not completely valid because the topography creates local variations of wind flow near the ground (Kaimal and Finnigan, 1994).

4.4.2 Bulk Richardson number

As it was explained before, sonic anemometry is not routinely used in wind energy, and bulk Richardson number Ri_b is an alternative way to estimate atmospheric stability based on a temperature difference and a single velocity level (Eq. (2)).

In Ri_b number equation, potential temperature Θ, is the temperature of an air parcel with absolute temperature T and pressure p would have if brought adiabatically to the pressure at the 1000 mb level. To first order it can be calculated as:

$$\Theta = T + \left(\frac{g}{C_p}\right)\Delta z \tag{5}$$

Where g is the acceleration due gravity, $Cp = 1000\ Jkg^{-1}K^{-1}$ is the specific heat capacity of the air at constant pressure, and Δz is the height difference from the 1000 mb level.

With Eq. (3) the obtained Ri_b will be used to estimates the stability parameter $\zeta = z/L$. As Bardal *et al.* (Bardal et al., 2018) explain, these formulations are only valid for values lower than 0.2, but to make a classification according to atmospheric stability they are considered adequate.

5.   Results and discussion

The study is divided into two parts: statistics of atmospheric stability with both methods (the Obukhov length and Richardson Bulk); and comparison between both methods.

5.1 Sonic method

Atmospheric boundary layer (ABL) models used in wind farm design tools are typically based on Monin-Obukhov theory. In stable conditions this surface-layer theory is extended to the entire ABL by assuming local scaling of turbulence characteristics through the stability parameter $\zeta = z/L$. This similarity theory would produce self-similar profiles of dimensionless quantities regardless of the height above ground level.

In the study case, as it was explained before, from the high-frequency (20 Hz) data recorded in the three available sonic anemometers in MP5 mast, the values of the Obukhov length (L) over a period of 10 minutes have been obtained, and taking into account the heights at which they are installed, the parameter $\zeta = z/L$.

In Fig. 4 the stability parameter $\zeta = z/L$ frequency distribution at the three sonic heights is depicted, resulting in showing a good agreement among them with a reduction of the percentage of conditions near neutral stability as the measurement height increases.

Comentario [ECN24]: Answer RC2 Technical corrections.

Con formato: Fuente: 10 pto, Sin Negrita, Inglés (Estados Unidos)

Comentario [ECN25]: Answer RC2 Technical corrections.

Comentario [ECN26]: Answer RC2 Technical corrections.

Con formato: Fuente: 10 pto, Sin Negrita

262

263
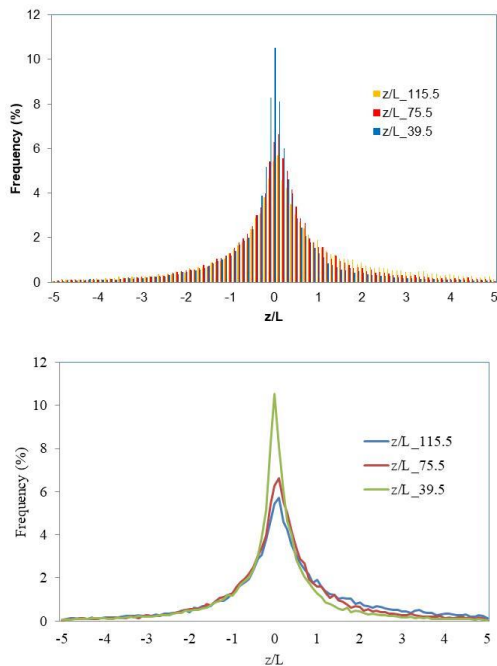
Figure 4 Probability distribution of z/L at all the sonic heights. Only concurrent time steps between July 2014 and June 2015 are included.

266   Figure 5 shows the distribution of atmospheric stability against wind speed at the MP5 measurements heights, the 9 stability classes propose in Table 1 are reduced to five combining: weakly unstable and stable classes with unstable and stable classes; and very unstable and stable with extremely unstable and stable. Table 3 shows the classification used. For the three heights, the stable situations are slightly higher than the unstable ones and there is an increase of neutral and stable conditions with increasing wind speeds, this is in accordance with the general knowledge that for strong wind speeds the atmosphere becomes neutrally stratified.

272

Table 3 According to Table 1 a reduced five stability classes.

Stability Class	Stability parameter $\zeta = z/L$
very unstable (vu)	$- \zeta < -0.6$
unstable (wu)	$-0.6 < \zeta < -0.02$
neutral (n)	$-0.02 < \zeta < 0.02$
stable (ws)	$0.02 < \zeta < 0.6$
very stable (vs)	$0.6 < \zeta$

273

274   As mentioned before, it is observed a significant dependence of stability distributions with height. At higher levels, the stability distributions are broader and there are more frequent cases with very large and extreme stability. This dependency of the stability distribution with height is because z is part of the definition of the stability parameter; and closer to the ground there are more "neutral" conditions because z/L tends to zero.

Comentario [ECN27]: Answer RC2 Specific comments

Comentario [ECN28]: Answer RC2 Technical corrections.

Comentario [ECN29]: Answer RC2 Technical corrections.

Comentario [ECN30]: Answer RC2 Technical corrections.

Comentario [ECN31]: Answer RC2 Technical corrections.
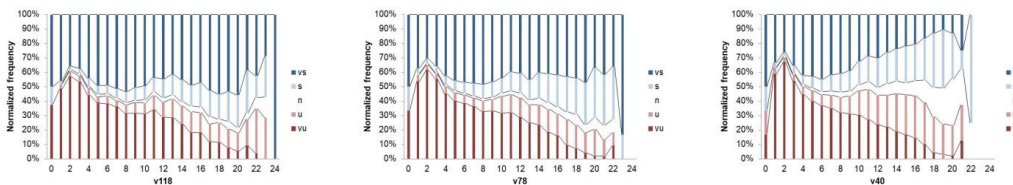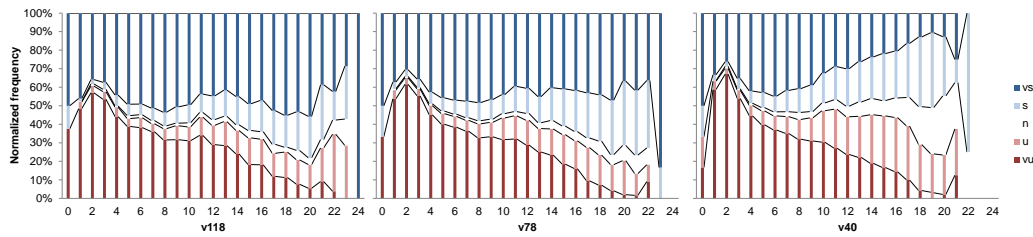
Comentario [ECN32]: Answer RC2 Specific comments

278 **Figure 5 Distribution of atmospheric stability with wind speed based on z/L obtained with sonic anemometer at different**
279 **heights, 115.5 m on the left, 75.5 m in the middle and 39.5 m on the right side. vs, very stable; s, stable; n, neutral; u,**
280 **unstable; vu, very unstable.**

281 The diurnal cycle, see Fig. 6, presents unstable conditions developing from 9.00 to 15.00. The rest of the day is
282 dominated by stable conditions resulting in low turbulence intensities.
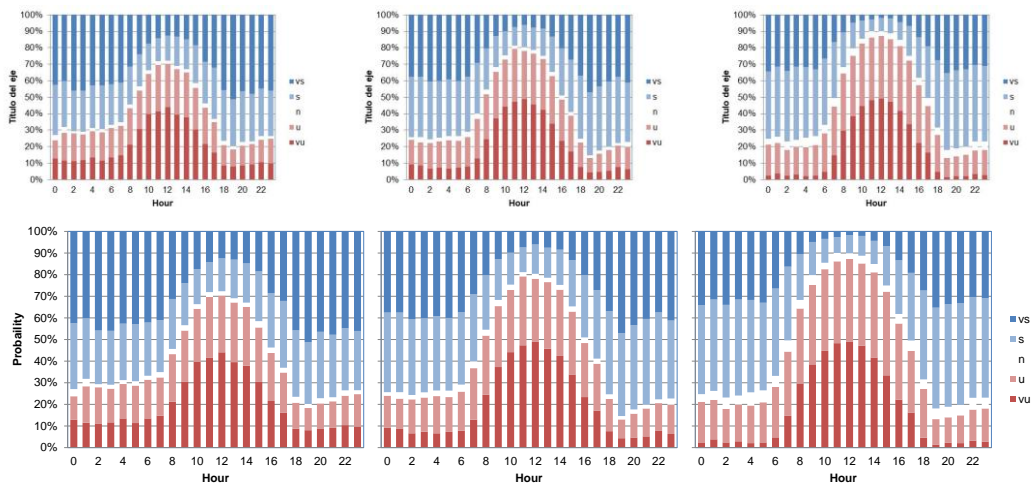
283 **Figure 6 Distribution of atmospheric stability with hour based on z/L obtained with sonic anemometer at different**
284 **heights, left 115.5 m, center 75.5m and right 39.5 m. vs, very stable; s, stable; n, neutral; u, unstable; vu, very unstable.**

285
286 Figure 7 shows the evolution of stability throughout the year. The stable side dominates during winter months,
287 with unstable conditions peaking between April to August where they take a ≈50% share.
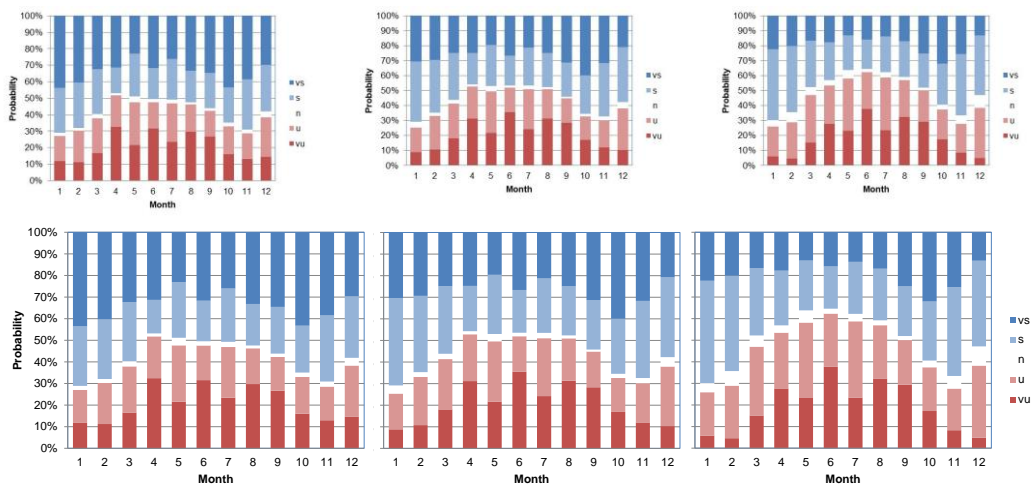
288 **Figure 7 Monthly distribution of stability based on z/L obtained with sonic anemometer at different heights, left 115.5**
289 **m, center 75.5 m and right 39.5 m. vs, very stable; s, stable; n, neutral; u, unstable; vu, very unstable.**

290   The variation of atmospheric stability with wind direction is showed in Fig. 8. Stable situations dominate in most
291 of the directions except for the northwest direction (330º-350º) that is one of the predominant in Alaiz. As can be
292 seen in Fig. 1, the North face of Alaiz Mountain has a steep slope (the Roughness Index (RIX) value in the north
293 sector in MP5 position is 22.4%) that empties into a large valley at around 700 m lower altitude. According to (Stull,
294 1989) this topography causes ascending hillside/valley winds that generate convective turbulence and therefore
295 situations of instability that could explain some of the unstable conditions found in the 330º-350º direction sector.
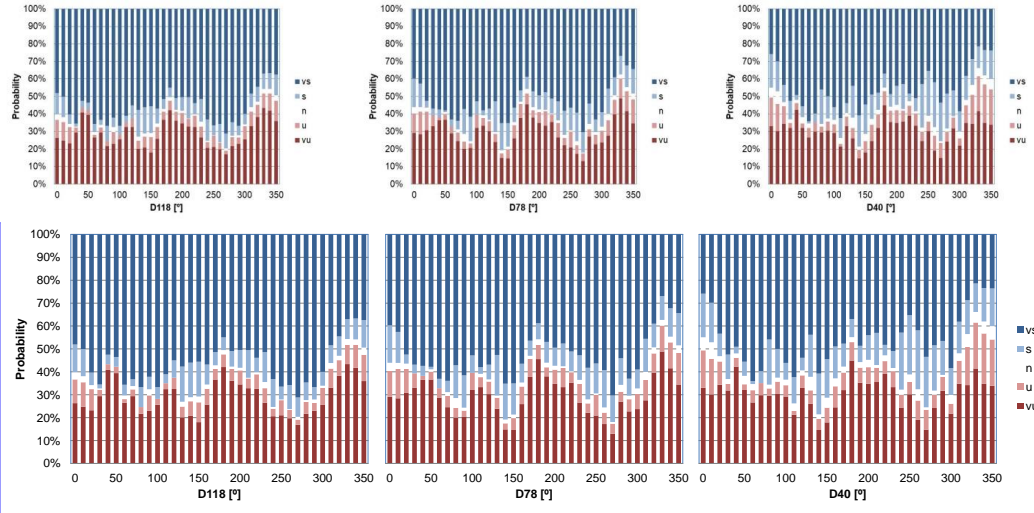
296 **Figure 8 Distribution of atmospheric stability with wind direction based on z/L obtained with sonic anemometer at**
297 **different heights. vs, very stable; s, stable; n, neutral; u, unstable; vu, very unstable.**

298
299   Following the stability classification defined in Table 3Table 1, Fig. 9 and Fig. 10 present the dependency of
300 wind shear (calculated as the wind speed ratio between 118 and 40 m) and turbulence intensity (calculated as the
301 ratio of the standard deviation to the mean wind speed at 118 m) with stability based on z/L parameter from the
302 three sonic sensors installed for the NNW and SSE prevailing wind direction sectors.
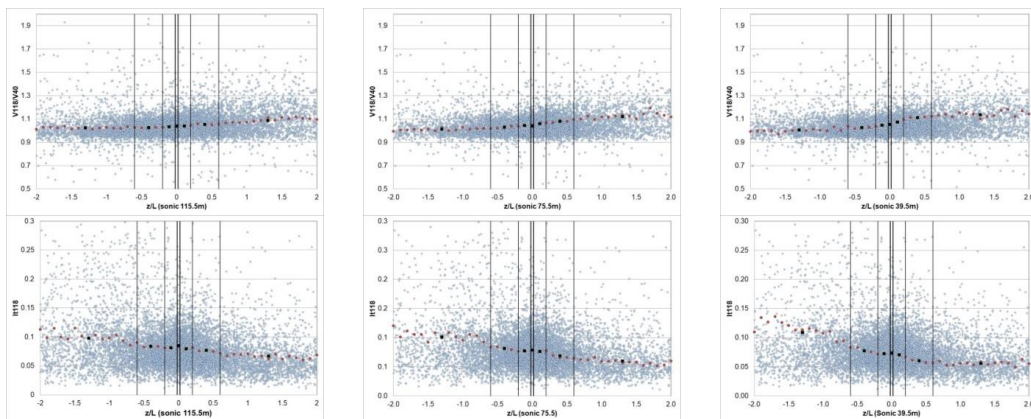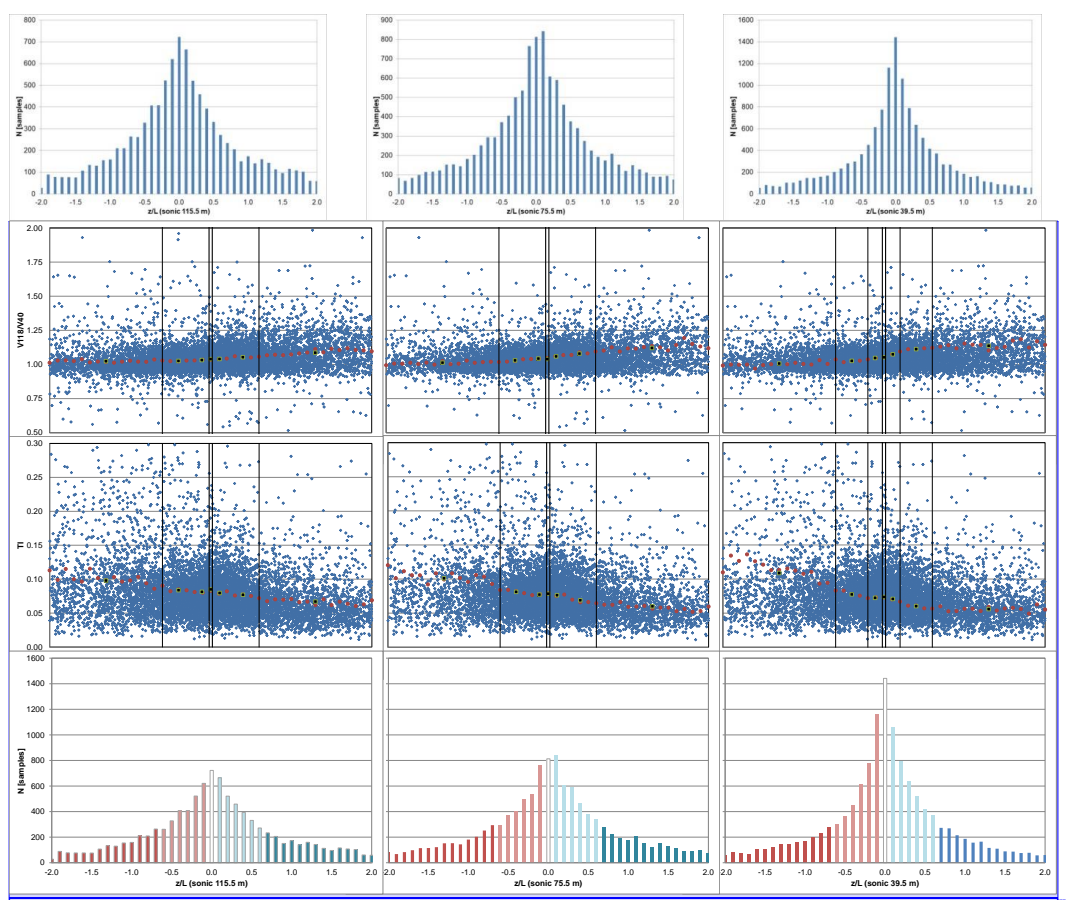
303   **Figure 9 Wind shear and turbulence intensity vs sonic stability in *MP5*, [337.5º-22.5º] sector. Red dots are the *z/L* mean**
304   **values for 0.01 resolution scale, black squares are the *z/L* mean values in each of the stability classes according to Table 1.**

305
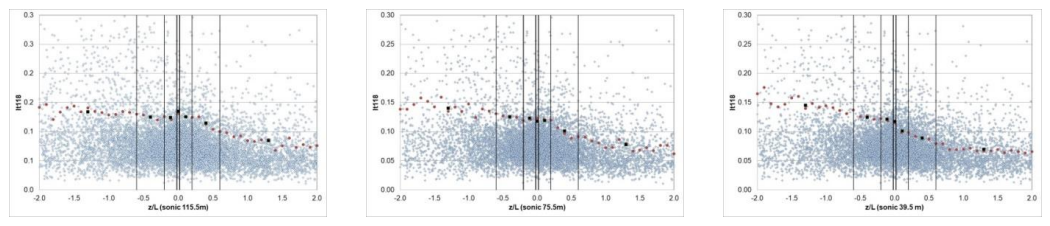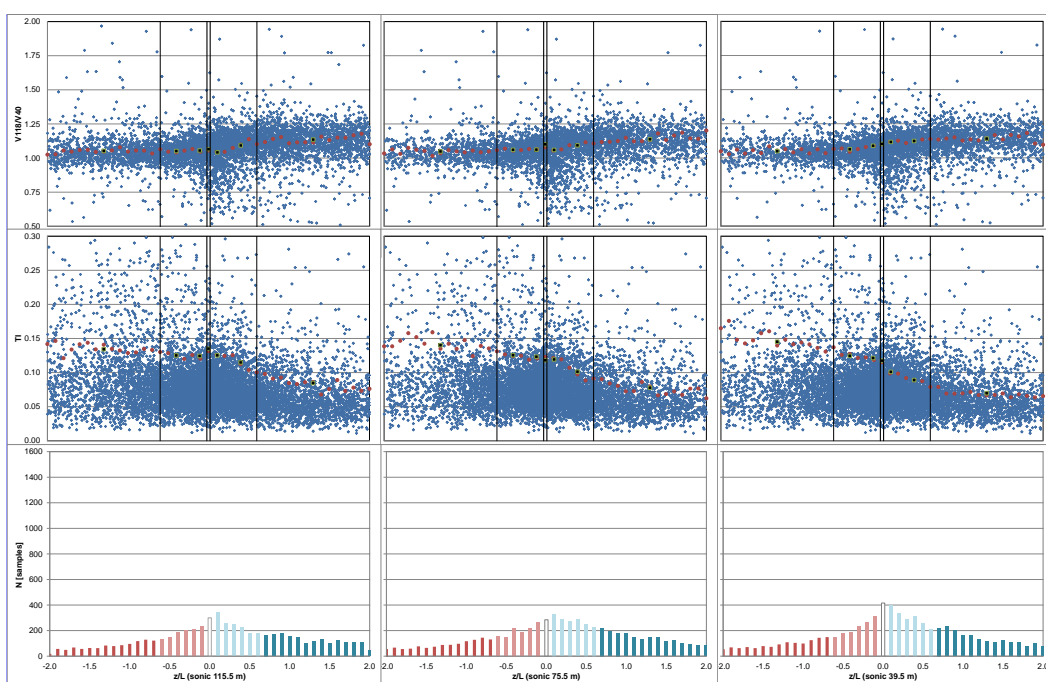
306 **Figure 10 Wind shear and turbulence intensity vs sonic stability in *MP5*, [157.5º-202.5º] sector. Red dots are the *z/L* mean**
307 **values for 0.01 resolution scale, black squares are the *z/L* mean values in each of the stability classes according to Table 1.**

308 For the three heights is observed that, as is explained by (Emeis, 2013), in unstable situations the ground surface is
309 warmer than the air above so there is a positive heat flux that causes more turbulence. This results in a convective,
310 well-mixed, surface layer with small vertical gradients. On the other hand, lower turbulence and high shear wind
311 profiles are associated to stable situations where turbulence is reduced due to a negative vertical heat flux.

312 **5.2 Bulk Richardson number**

313 Since sonic anemometers are not commonly used in wind resource assessment, an alternative method to estimate the
314 atmospheric stability is Bulk Richardson number. It is based on mean wind speed at height z and mean virtual
315 potential temperature difference between air at the reference height (z) and surface temperature.

316 The calculation of the Bulk–Richardson number is, in the present study, not straightforward because of the lack
317 of reliable sensors at the surface. The lower air temperature is measured at 2 m in MP5 mast. Ideally, the
318 temperature difference at the air-surface interface is required (Kaimal and Finnigan, 1994) for stability analysis.
319 However, because of the lack of surface temperature, 2 m height air temperature has been chosen as representative.
320 Observations of 118 m wind speed and 113 m air temperature have been used in conjunction with 2 m air
321 temperature to estimate Ri_b.

322 ~~As in the work that is presented in some measurement campaigns, there are no~~The MP5 mast has not
323 measurements of surface temperature or near the ground. Some authors in these circumstances either extrapolate the
324 values to the surface (z=0) (Machefaux et al., 2016) or perform the calculation directly between the available
325 temperature levels (Martin et al., 2016; Ruisi and Bossanyi, 2019; Zhan et al., 2020). To analyze how the choice of
326 measurement heights may influence resulting Ri_b stability distributions the Ri_b has also been calculated using 38 m
327 air temperature instead 2 m.

328 The values of the Bulk-Richardson number have been obtained over a period of 10 minutes, i.e. the same period
329 used for calculation of the Obukhov length.

330 Figure 11 shows the distribution for the bulk Richardson number method. The lower measurement level is varied
331 between 2 and 38 m. Using the 38 m level, it is observed that according to the classification in Table 2, unstable
332 cases practically disappear. This is not physically possible and does not occur in the classification obtained by the
333 sonic method (see Fig. 4). So In this case, the results obtained using the 38 m temperature sensor as a representative
334 surface level ~~does~~ not give us any reliable information. Small temperature differences highly affect the result of the
335 Richardson number method and therefore it is greatly affected by deviations in the measurement of this variable.

The MP5 temperature sensors have an accuracy of 0.3 ℃ and the mean temperature difference in the period analyzed between the level of 38 m and that of 113 m has been 0.7 ℃ so the uncertainty of the measurement is of the same order as the measurement itself.

The selection of temperature measurement heights has a great effect on the bulk Richardson number method, both in the exactitude and in the applicability of the method. To reduce uncertainties the measurements should be made either with differential temperature sensors or with calibrated sensors and a sufficient vertical separation in order to reduce the influence of inaccuracies in the temperature measurements (Baker and Bowen, 1989; Brower, 2012).
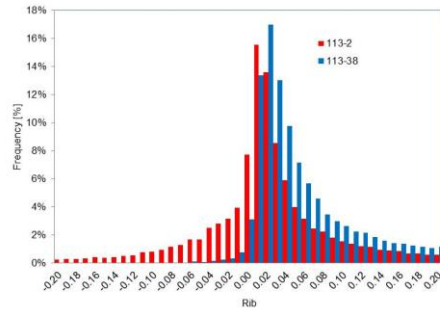
Figure 11 Probability distribution of Ri$_b$ measured between 2 m and 113 (red one) and between 38 and 113 m (blue lines). Only concurrent time steps between July 2014 and June 2015 are included.

Figure 12 shows the distribution of atmospheric stability against wind speed. On the left side atmospheric stability is directly classified with the Ri$_b$ obtained with observations of 118 m wind speed, 113 m air temperature and 2 m air temperature, this last temperature sensor has been chosen as representative of surface temperature. The seven stability classes propose in Table 2 are reduced to five combining: weakly unstable and /stable classes with unstable and /stable classes. Table 4 shows the classification used. On the right side atmospheric stability is classified according to the stability parameter $\zeta = z/L$ obtained with Ri$_b$ and Eq. (3(3) and according to stability classification proposed in Table 3. The nine stability classes propose in Table 1 are reduced to five combining: weakly un/stable classes with un/stable classes; and very un/stable with extremely un/stable.

Table 4 According to Table 2 a reduced five stability classes

Stability Class	Stability parameter Ri$_b$
Very unstable	Rib < -0.023
Unstable	-0.023 < Rib < -0.0036
Neutral	-0.0036 < Rib < 0.0072
Stable	0.0072 ≤ Rib > 0.084
Very stable	Rib > 0.084

Both distributions show a differentiated behavior with fewer "very" unstable and /stable situations and a greater number of neutral observations in the case of the classification with ζ (on the right side of Fig. 12).

Comentario [ECN45]: Answer RC2 Technical corrections.

Comentario [ECN46]: Answer RC2 Technical corrections.

Con formato: Fuente: 10 pto, Sin Negrita

Comentario [ECN47]: Answer RC2 Technical corrections.

Comentario [ECN48]: Answer RC2 specific comments

Comentario [ECN49]: Answer RC2 Technical corrections.
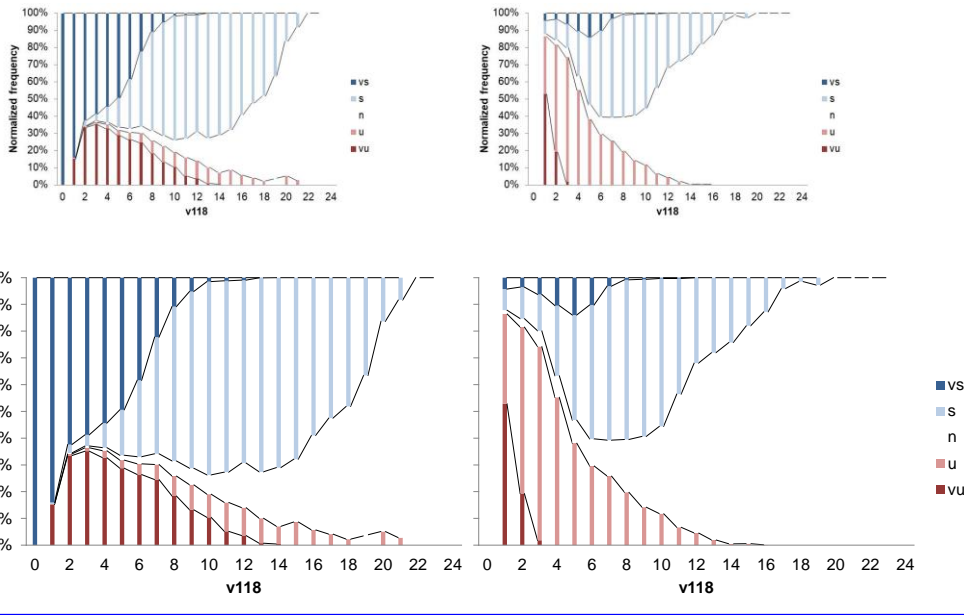
361 **Figure 12 Distribution of atmospheric stability with wind speed. On the left based on Rib; On the right based on z/L**
362 **obtained from Rib with transformation functions by Businger and Dyer. vs, very stable; s, stable; n, neutral; u,**
363 **unstable; vu, very unstable.**

5.3 Comparison of stability methods: sonic versus bulk method

365 Comparing the distribution of atmospheric stability against wind speed based on sonic method (Fig. 5) with the
366 results obtained based on Ri_b method (Fig. 12); it is observed that there are important differences between them.

367 Table 5~~Table 3~~ presents a frequency of occurrence of stability classes with concurrent data using different
368 methods. This quantitative comparison shows that taking the sonic method as benchmark, it is observed that the bulk
369 method when the Businger and Dyer functions are used to estimate the stability parameter $\zeta = z/L$ over predict the
370 percentage of neutral and stable conditions to the detriment of very unstable and stable situations, probably due to
371 similar air temperature values at 113 an 2 m. On the other hand, classification directly with Rib according to Mohan
372 classification over predict too the stable situations at the cost of under predicting the unstable ones. As is explained
373 in some references (Bardal et al., 2018; Sathe et al., 2011), stability characterization with Ri_b have several weak
374 points: in one hand Ri_b method is sensitive to temperature measurements and uncertainty in L estimation increases
375 as the temperature difference is reduced. Besides, other source of uncertainty comes from the definition of the
376 surface temperature. In the other hand Businger and Dyer functions have some limitations and as ~~Bardal *et al.*~~
377 ~~propose in~~ (Bardal et al., 2018) propose the use of more advanced methods for relating the Ri_b to ~~de~~ the z/L
378 parameter might improve the results.

379 Besides these methodological reasons there are some physical causes of the differences found. One of these is
380 that Richardson bulk number represents a bulk average stability value instead a local measurement like the sonic
381 method.

382 ~~Table 3~~Table 5 **Frequency of occurrence of stability classes.**

	115.5/L	75.5/L	39.5/L	z/L from Ri_b	Ri_b
vu	21.2%	21.3%	19.9%	0.7%	18.1%
u	19.4%	21.4%	26.8%	21.2%	5.9%
n	2.2%	2.4%	4.4%	32.5%	8.2%
s	24.0%	28.2%	29.9%	42.2%	43.6%
vs	33.2%	26.7%	19.1%	3.5%	24.2%

Comentario [ECN50]: Answer RC2 specific comments

Comentario [ECN51]: Answer RC2 Technical corrections.

Comentario [ECN52]: Answer RC2 Technical corrections.

6. Conclusions

In this work, a detailed data analysis focused on how to estimate atmospheric stability in a site with complex terrain was presented. The Obukhov parameter $\zeta = z/L$, which can be measured locally with the use of a sonic anemometer, and bulk Richardson number have been studied. The methods are examined considering their theoretical background, implementation complexity, instrumentation requirements, and practical use in connection with wind energy applications.

It is shown that the resulting stability depends on which method is chosen. The sonic method is ~~taking~~ taken as benchmark because is the only way of measuring local stability without the use of empirical functions or theoretical assumptions. However this method requires working with accurate high frequency data, rotating the measurements to align the coordinate system to the mean wind vector, which is reported to require special attention in complex terrain to guarantee that the mean streamline plane will be parallel to the terrain surface; to finally obtain turbulent fluxes using the eddy covariance technique.

According to the stability parameter $\zeta = z/L$ obtained with the three sonic anemometer installed in MP5 mast. For the three heights, the stable situations are slightly higher than the unstable ones and there is an increase of neutral and stable conditions with increasing wind speeds. There is a significant dependence of stability distributions with height. At higher levels, the stability distributions are broader and there are more frequent cases with very large and extreme stability.

The seasonal and diurnal cycle is identified, in the winter and during the hours between 17h to 8h stable side dominates, while between April to August and between 9h to 15h unstable conditions are found to be more frequent. Winds from the predominant northwest direction (330º-350º) produce more unstable conditions than the others sectors.

For the three heights, and in the two predominant sectors, is observed that in in unstable situations the ground surface is warmer than the air above so there is a positive heat flux that causes more turbulence. This results in a convective, well-mixed, surface layer with small vertical gradients. On the other hand, lower turbulence and high shear wind profiles are associated to stable situations where turbulence is reduced due to a negative vertical heat flux.

As alternative to characterize stability, the bulk Richardson number is explored, it requires the minimum level of instrumentation, mean wind speed at height z and mean virtual potential temperature difference between air at the reference height (z) and surface temperature. The bulk Richardson number can be used directly to ~~classified~~ classify the atmospheric stability or it can be transform into $\zeta = z/L$ by Businger and Dyer functions.

On MP5 there is not a surface temperature sensor so 2 m high air temperature sensor has been chosen as representative, moreover to analyze how the choice of measurement heights may influence resulting Ri_b stability distributions, it has also been calculated using 38 m air temperature sensor instead 2 m. This configuration does not give us any reliable information, it could be due temperature sensors on MP5 have an accuracy of 0.3ºC and the mean temperature difference in the period analyzed between the level of 38 m and that of 113 m has been 0.7 ºC so the uncertainty of the measurement is of the same order as the measurement itself. The Ri_b number relies on smaller temperature differences for estimation of the mean gradient and its accuracy is therefore dependent on the sensor precision, calibration and measurement heights. The following recommendations are provided to obtain consistent results with bulk Richardson method: use high precision temperature sensors; calibrate all the temperature sensors at the same time; calibrate the temperature sensors in the operational range to guarantee better calibration in the temperatures of interest and have a reference temperature sensor below 2 m, as close to the ground as possible.

On the other hand, the stability classification obtained using directly the Ri_b values shows a differentiated behavior than that estimated according to the stability parameter $\zeta = z/L$ obtained with Ri_b and Businger and Dyer functions. It could be by the different classification employed in both characterization (Mohan vs Sorbjan & Grachev) and/or by the Businger and Dyer functions.

In summary the sonic method is more costly and complex but, in this study, it shows results in accordance with the general atmospheric boundary layer knowledge, so we recommend it at as first option to obtain a local measurement of atmospheric stability that can be associated to a certain height above the ground. For the Bulk Richardson number, based in the references read, there ~~isn't~~ is no a standard methodology for characterizing atmospheric stability using this method and there are many different approximations. Furthermore, empirical relations to relate Ri_b to $\zeta = z/L$ are obtained either for offshore sites or for non-complex sites, so there is a need for observational studies on complex terrain to increase under-standing of how estimate atmospheric stability accurately with Bulk Richardson number.

Data availability. Data belongs to CENER and it ~~could~~ can be obtained from the author upon request.

Author contribution. EC is the principal investigator of the project and coordinated the activities and the preparation of the paper. DP aided in the formulation of the scope of the work, FB assisted in the measurement post-processing, while the methodology was devised by EC, JS and DP. The stability analysis and visualization was performed by EC. EC wrote the original draft, AG helped with the composition of the manuscript while EC, JSR, FB, DP and AG contributed, reviewed and edited the final paper.

Competing interests. The authors declare that they have no conflict of interest.

Acknowledgements. The authors are grateful to CENER for sharing the MP5 database with us during the course of this research. ~~The authors are grateful to CENER for sharing the MP5 database and to~~

References

Abkar, M. and Porté-Agel, F.: Influence of atmospheric stability on wind-turbine wakes: A large-eddy simulation study, Phys. Fluids, 27(3), 35104, doi:10.1063/1.4913695, 2015.

Aubinet, M., Vesala, T. and Papale, D.: Eddy Covariance : A practical guide to measurement and data analysis., 2012.

Baker, B. and Bowen, J.: Quality Assurance Handbook for Air Pollution Measurement Systems: Volume IV : Meteorological Measurements., 1989.

Bardal, L. M., Onstad, A. E., Sætran, L. R. and Lund, J. A.: Evaluation of methods for estimating atmospheric stability at two coastal sites, Wind Eng., 42(6), 561–575, doi:10.1177/0309524X18780378, 2018.

Brower, M. C.: WIND RESOURCE ASSESSMENT: A Practical Guide to Developing a Wind Project., 2012.

Burba, G.: Eddy Covariance Method for Scientific, Industrial, Agricultural and Regulatory Applications., 2013.

Burba, G. and Anderson, D.: Eddy Covariance Flux Measurements. [online] Available from: http://www.ncbi.nlm.nih.gov/pubmed/18767616, 2010.

Cuerva, A., Sanz-Andrés, A. and Navarro, J.: On multiple-path sonic anemometer measurement theory, Exp. Fluids, 34(3), 345–357, doi:10.1007/s00348-002-0565-x, 2003.

Cuerva, A., Sanz-Andrés, A., Franchini, S., Eecen, P., Busche, P., Pedersen, T. F. and Mouzakis, F.: ACCUWIND: Task 2. Improve the Accuracy of Sonic Anemometers., 2006.

Dyer, A. J.: A review of flux-profile relationships, Boundary-Layer Meteorol., 7(3), 363–372, doi:10.1007/BF00240838, 1974.

Emeis, S.: Wind Energy Meteorology Atmospheric Physics for Wind Power Generation (Green Energy and Technology), First Edit., Springer, Berlin, Heidelberg., 2013.

Finnigan, J., Ayotte, K., Harman, I., Katul, G., Oldroyd, H., Patton, E., Poggi, D., Ross, A. and Taylor, P.: Boundary-Layer Flow Over Complex Topography, Boundary-Layer Meteorol., 177(2–3), 247–313, doi:10.1007/s10546-020-00564-3, 2020.

Foken, T.: 50 years of the Monin-Obukhov similarity theory, Boundary-Layer Meteorol., 119(3), 431–447, doi:10.1007/s10546-006-9048-6, 2006.

Geissbühler, P., Siegwolf, R. and Eugster, W.: Eddy Covariance Measurements On Mountain Slopes: The Advantage Of Surface-Normal Sensor Orientation Over A Vertical Set-Up, Boundary-Layer Meteorol., 96(3), 371–392, doi:10.1023/A:1002660521017, 2000.

Grachev, A. A. and Fairall, C. W.: Dependence of the M-O stability parameters on the Bulk Ri over the ocean, J. Appl. Meteorol., 36, 406–415, doi:10.1175/1520-0450(1997)036<0406:DOTMOS>2.0.CO;2, 1997.

Han, X., Liu, D., Xu, C. and Shen, W. Z.: Atmospheric stability and topography effects on wind turbine performance and wake properties in complex terrain, Renew. Energy, 126, 640–651, doi:10.1016/j.renene.2018.03.048, 2018.

Hansen, K. H., Barthelmie, R. J., Jensen, L. E. and Sommer, A.: The impact of turbulence intensity and atmospheric stability on power deficits due to wind turbine wakes at Horns Rev wind farm., Wind Energy, 15, 183–196, 2010.

IEC61400-1 (ED4) 2019: IEC61400-1 ed.4, Wind energy generation systems - Part 1: Design requirements. [online] Available from: https://webstore.iec.ch/publication/26423 (Accessed 16 April 2021), 2019.

IEC61400-12-1 (ED1) 2005-12: IEC61400-12-1 ed1., Wind turbines- Part 12-1: Power performance measurements

484   of electricity producing wind turbines., 2005.

485   Kaimal, J. C. and Businger, J. a.: A Continuous Wave Sonic Anemometer-Thermometer, J. Appl. Meteorol., 2(1),
486   156–164, doi:10.1175/1520-0450(1963)002<0156:ACWSAT>2.0.CO;2, 1963.

487   Kaimal, J. C. and Finnigan, J. J.: Atmospheric Boundary Layer Flows: Their Structure and Measurement, 1st ed.,
488   Oxford University Press., 1994.

489   Kaimal, J. C. and Gaynor, J. E.: Another look at sonic thermometry, Boundary-Layer Meteorol., 56(4), 401–410,
490   doi:10.1007/BF00119215, 1991.

491   Kelly, M., Larsen, G., Dimitrov, N. K. and Natarajan, A.: Probabilistic Meteorological Characterization for Turbine
492   Loads, J. Phys. Conf. Ser., 524, 012076, doi:10.1088/1742-6596/524/1/012076, 2014.

493   Lange, B., Larsen, S., Højstrup, J. and Barthelmie, R.: Importance of thermal effects and sea surface roughness for
494   offshore wind resource assessment, J. Wind Eng. Ind. Aerodyn., 92(11), 959–988, doi:10.1016/j.jweia.2004.05.005,
495   2004a.

496   Lange, B., Larsen, S., Højstrup, J. and Barthelmie, R.: The Influence of Thermal Effects on the Wind Speed Profile
497   of the Coastal Marine Boundary Layer, Boundary-Layer Meteorol., 112(3), 587–617,
498   doi:10.1023/B:BOUN.0000030652.20894.83, 2004b.

499   Machefaux, E., Larsen, G. C., Koblitz, T., Troldborg, N., Kelly, M. C., Chougule, A., Hansen, K. S. and Rodrigo, J.
500   S.: An experimental and numerical study of the atmospheric stability impact on wind turbine wakes, Wind Energy,
501   19(10), 1785–1805, doi:https://doi.org/10.1002/we.1950, 2016.

502   Martin, C. M. S., Lundquist, J. K., Clifton, A., Poulos, G. S. and Schreck, S. J.: Wind turbine power production and
503   annual energy production depend on atmospheric stability and turbulence, Wind Energy Sci., 1(2), 221–236,
504   doi:10.5194/wes-1-221-2016, 2016.

505   Measnet: MEASNET Procedure: Anemometer Calibration, Version 2, October 2009. [online] Available from:
506   http://www.measnet.com/wp-content/uploads/2011/06/measnet_anemometer_calibration_v2_oct_2009.pdf, 2009.

507   Mohan, M.: Analysis of various schemes for the estimation of atmospheric stability classification, Atmos. Environ.,
508   32(21), 3775–3781, doi:10.1016/S1352-2310(98)00109-5, 1998.

509   Monin, A. S. and Obukhov, A. M.: Basic laws of turbulent mixing in the atmosphere near the ground, Tr. Akad.
510   Nauk SSSR Geofiz. Inst, 24, 163–187, 1954.

511   Peña, A. and Hahmann, A. N.: Atmospheric stability and turbulence fluxes at Horns Rev—an intercomparison of
512   sonic, bulk and WRF model data, Wind Energy, 15(5), 717–731, doi:https://doi.org/10.1002/we.500, 2012.

513   Radünz, W. C., Sakagami, Y., Haas, R., Petry, A. P., Passos, J. C., Miqueletti, M. and Dias, E.: The variability of
514   wind resources in complex terrain and its relationship with atmospheric stability, Energy Convers. Manag.,
515   222(July), 113249, doi:10.1016/j.enconman.2020.113249, 2020.

516   Radünz, W. C., Sakagami, Y., Haas, R., Petry, A. P., Passos, J. C., Miqueletti, M. and Dias, E.: Influence of
517   atmospheric stability on wind farm performance in complex terrain, Appl. Energy, 282(PA), 116149,
518   doi:10.1016/j.apenergy.2020.116149, 2021.

519   Richiardone, R., Giampiccolo, E., Ferrarese, S. and Manfrin, M.: Detection of Flow Distortions and Systematic
520   Errors in Sonic Anemometry Using the Planar Fit Method, Boundary-Layer Meteorol., 128(2), 277–302,
521   doi:10.1007/s10546-008-9283-0, 2008.

522   Ruisi, R. and Bossanyi, E.: Engineering models for turbine wake velocity deficit and wake deflection. A new
523   proposed approach for onshore and offshore applications, J. Phys. Conf. Ser., 1222(1), doi:10.1088/1742-
524   6596/1222/1/012004, 2019.

525   Santos, P., Mann, J., Vasiljević, N., Cantero, E., Sanz Rodrigo, J., Borbón, F., Mart\'\inez-Villagrasa, D., Mart\'\i,
526   B. and Cuxart, J.: The Alaiz experiment: untangling multi-scale stratified flows over complex terrain, Wind Energy
527   Sci., 5(4), 1793–1810, doi:10.5194/wes-5-1793-2020, 2020.

528   Sanz Rodrigo, J.: Flux-profile characterization of the offshore ABL for the parameterization of CFD models, EWEA
529   offshore, 2011.

530   Sanz Rodrigo, J., Borbón Guillén, F., Gómez Arranz, P., Courtney, M. S., Wagner, R. and Dupont, E.: Multi-site
531   testing and evaluation of remote sensing instruments for wind energy applications, Renew. Energy, 53, 200–210,
532   doi:10.1016/j.renene.2012.11.020, 2013.

533   Sanz Rodrigo, J., Cantero, E., García, B., Borbón, F., Irigoyen, U., Lozano, S., Fernande, P. M. and Chávez, R. A.:

534   Atmospheric stability assessment for the characterization of offshore wind conditions, J. Phys. Conf. Ser., 625,
535   012044, doi:10.1088/1742-6596/625/1/012044, 2015.

536   Sathe, A., Gryning, S.-E. and Peña, A.: Comparison of the atmospheric stability and wind profiles at two wind farm
537   sites over a long marine fetch in the North Sea, Wind Energy, 14(6), 767–780, doi:10.1002/we.456, 2011.

538   Sathe, A., Mann, J., Barlas, T., Bierbooms, W. A. A. M. and van Bussel, G. J. W.: Influence of atmospheric stability
539   on wind turbine loads, Wind Energy, 16(7), 1013–1032, doi:https://doi.org/10.1002/we.1528, 2013.

540   Schmidt, J., Chang, C.-Y., Dörenkämper, M., Salimi, M., Teichmann, T. and Stoevesandt, B.: The consideration of
541   atmospheric stability within wind farm AEP calculations, J. Phys. Conf. Ser., 749, 012002, doi:10.1088/1742-
542   6596/749/1/012002, 2016.

543   Schotanus, P., Nieuwstadt, F. T. M. and Bruin, H. A. R.: Temperature measurement with a sonic anemometer and its
544   application to heat and moisture fluxes, Boundary-Layer Meteorol., 26(1), 81–93, doi:10.1007/BF00164332, 1983.

545   Sorbjan, Z. and Grachev, A. A.: An Evaluation of the Flux--Gradient Relationship in the Stable Boundary Layer,
546   Boundary-Layer Meteorol., 135(3), 385–405, doi:10.1007/s10546-010-9482-3, 2010.

547   Stiperski, I. and Rotach, M. W.: On the Measurement of Turbulence Over Complex Mountainous Terrain,
548   Boundary-Layer Meteorol., 159(1), 97–121, doi:10.1007/s10546-015-0103-z, 2015.

549   Stull, R. B.: An Introduction to Boundary Layer Meteorology, Springer Netherlands., 1989.

550   Wilczak, J. M., Oncley, S. P. and Stage, S. A.: Sonic Anemometer Tilt Correction Algorithms, Boundary-Layer
551   Meteorol., 99(1), 127–150, doi:10.1023/A:1018966204465, 2001.

552   Zhan, L., Letizia, S. and Valerio Iungo, G.: LiDAR measurements for an onshore wind farm: Wake variability for
553   different incoming wind speeds and atmospheric stability regimes, Wind Energy, 23(3), 501–527,
554   doi:https://doi.org/10.1002/we.2430, 2020.

555